

Fernanda Marques · Krassimira P. Guerra · Lurdes Gano · Judite Costa · M. Paula Campello
Luís M. P. Lima · Rita Delgado · Isabel Santos

^{153}Sm and ^{166}Ho complexes with tetraaza macrocycles containing pyridine and methylcarboxylate or methylphosphonate pendant arms

Received: 11 May 2004 / Accepted: 27 July 2004 / Published online: 28 August 2004
© SBIC 2004

Abstract A set of tetraaza macrocycles containing pyridine and methylcarboxylate ($\text{ac}_3\text{py}14$) or methylphosphonate ($\text{MeP}_2\text{py}14$ and $\text{P}_3\text{py}14$) pendant arms were prepared and their stability constants with La^{3+} , Sm^{3+} , Gd^{3+} and Ho^{3+} determined by potentiometry at 25 °C and 0.10 M ionic strength in NMe_4NO_3 . The metal:ligand ratio for ^{153}Sm and ^{166}Ho and for $\text{ac}_3\text{py}14$, $\text{MeP}_2\text{py}14$ and $\text{P}_3\text{py}14$, as well as the pH of the reaction mixtures, were optimized to achieve a chelation efficiency higher than 98%. These radiocomplexes are hydrophilic and have a significant plasmatic protein binding. In vitro stability was studied in physiological solutions and in human serum. All complexes are stable in saline and PBS, but 20% of radiochemical impurities were detected after 24 h of incubation in serum. Bio-distribution studies in mice indicated a slow rate of clearance from blood and muscle, a high and rapid liver uptake and a very slow rate of total radioactivity excretion. Some bone uptake was observed for complexes with $\text{MeP}_2\text{py}14$ and $\text{P}_3\text{py}14$, which was enhanced with time and the number of methylphosphonate groups. This biological profile supports the in vitro instability found in serum and is consistent with the thermodynamic stability constants found for these complexes.

Keywords Lanthanides · Pendant arms · Radiopharmaceuticals · Stability constants · Tetraaza macrocycles

Introduction

Therapeutic radiopharmaceuticals are rapidly developing as an additional treatment modality in oncology and a variety of radionuclides has been exploited for their therapeutic potential [1, 2, 3, 4]. Recently, new therapeutic radiopharmaceuticals have been introduced with the objective of delivering large radiation doses to the diseased sites while sparing normal cells and normal tissues [5, 6, 7]. This is mainly due to the development of a range of carrier biomolecules, monoclonal antibodies [8, 9, 10, 11] and peptides [12, 13, 14, 15], which can target radionuclides more selectively to the disease site, and also due to the wider availability of radionuclides with desired physical properties [16, 17, 18, 19, 20]. ^{153}Sm and ^{166}Ho are attractive candidates for therapeutic applications due to their favorable chemistry and physical characteristics [21, 22, 23, 24, 25]. Nevertheless, developments in radionuclide therapy have not been confined to proteins and peptides. Another active research area is related to the development of bone pain palliation radiopharmaceuticals [26, 27].

Macrocyclic chelators, namely 12- to 14-membered tetraaza macrocycles with methylcarboxylate and/or methylphosphonate arms, have been proposed as bifunctional agents for labeling antibodies and peptides and as agents for targeted radionuclide therapy [28]. It has been shown that structural factors, such as cavity size, rigidity of the macrocyclic backbone, type and position of donor atoms, play a significant role in the binding features of the macrocycles and on the stability and kinetic inertness of the complexes [29, 30, 31]. The 12-membered *dota* (1,4,7,10-tetraazacyclododecane-1,4,7,10-tetraacetic acid) and the 14-membered *teta* (1,4,8,11-tetraazacyclotetradecane-1,4,8,11-tetraacetic acid)

F. Marques (✉) · L. Gano · M. P. Campello · I. Santos
Instituto Tecnológico e Nuclear, Estrada Nacional 10,
2686-953 Sacavém, Portugal
E-mail: fmarujo@itn.mces.pt

K. P. Guerra · J. Costa · L. M. P. Lima · R. Delgado
Instituto de Tecnologia Química e Biológica, UNL,
Apartado 127, 2781-901 Oeiras, Portugal

J. Costa
Faculdade de Farmácia, Universidade de Lisboa,
Av. das Forças Armadas, 1600 Lisbon, Portugal

R. Delgado
Instituto Superior Técnico, Av. Rovisco Pais,
1049-001 Lisbon, Portugal

form thermodynamically stable and kinetically inert complexes with divalent and trivalent metal cations [32]. Radiolabeled macrocycles with methylphosphonate substituents, such as $^{153}\text{Sm}/^{166}\text{Ho}$ -dotp, have already been evaluated as bone-seeking radiopharmaceuticals, but the exact mechanism for bone uptake is poorly understood [23, 33]. Nevertheless, it is well known that complexes of ligands containing phosphonate arms are very effectively retained in the bone and calcified tissues and tend to localize on the surface of hydroxyapatite crystals (the main bone component) [33, 34]. However, Kim et al. [35, 36] have also found considerable *in vivo* bone uptake for cationic lanthanide complexes with macrocyclic methylcarboxylate ligands containing one or two pyridines. Recently, Aimé et al. [37, 38, 39] studied complexes of 12- to 14-membered tetraaza macrocycles containing pyridine and bearing acetate and/or methylphosphonate arms with La(III), Gd(III) and Lu(III) for NMR applications. They found that the thermodynamic stability was dictated by the size of the lanthanide ion and by the cavity size of the macrocycle.

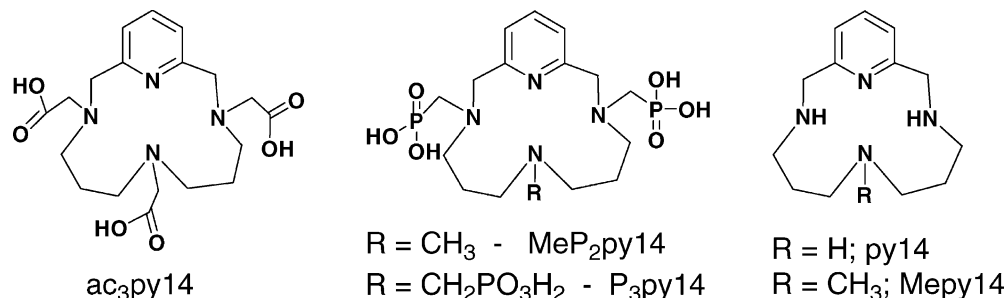
Considering that the introduction of a pyridine moiety in the macrocyclic backbone is expected to increase the stereochemical rigidity of the resulting complexes, to provide functionalization towards specific targets and to allow the formation of neutral complexes with Ln^{3+} , we decided to study 14-membered tetraaza macrocycles containing pyridine and methylcarboxylate ($\text{ac}_3\text{py14}$) or methylphosphonate ($\text{MeP}_2\text{py14}$, $\text{P}_3\text{py14}$) pendant arms (Fig. 1). These studies were performed with La^{3+} , Sm^{3+} , Gd^{3+} and Ho^{3+} , aiming at radiopharmaceutical applications. Herein, we report on the stability constants of $\text{ac}_3\text{py14}$, $\text{MeP}_2\text{py14}$ and $\text{P}_3\text{py14}$ with those lanthanide ions and also on the synthesis and biological evaluation of the complexes prepared with ^{153}Sm and ^{166}Ho .

Materials and methods

Materials

Enriched Sm_2O_3 (98.4% ^{152}Sm) was purchased from Campro Scientific and natural Ho_2O_3 (99.9%) from Strem. All the macrocyclic compounds were synthesized and purified according to methods previously reported [40, 41, 42]. All materials were reagent grade unless otherwise specified.

Fig. 1 Structures of the three macrocyclic ligands containing methylcarboxylate ($\text{ac}_3\text{py14}$), methyl ($\text{MeP}_2\text{py14}$) and methylphosphonate ($\text{P}_3\text{py14}$) pendant arms used in this study. The parent macrocycles, py14 and Mepy14 , are also represented



Potentiometric measurements

Reagents and solutions

Lanthanide ion solutions were prepared at 0.025–0.050 M from the nitrate salts of the analytical grade metals with demineralized water (from a Millipore/Milli-Q system), and were kept in excess nitric acid to prevent hydrolysis. Solutions were standardized by titration with $\text{Na}_2\text{H}_2\text{edta}$ [43]. The carbonate-free solution of the titrant, NMe_4OH , was prepared by treating freshly prepared silver oxide with a solution of NMe_4I under nitrogen [44]. Solutions were discarded when carbonate was about 0.5% of the total amount of base [45, 46]. For the back titrations a 0.100 M HNO_3 solution was used.

Equipment and work conditions

The equipment used was described previously [40, 41, 42]. The temperature was kept at 25.0 ± 0.1 °C; atmospheric CO_2 was excluded from the cell during the titration by passing purified nitrogen across the top of the experimental solution in the reaction cell. The ionic strength of the solutions was kept at 0.10 M with NMe_4NO_3 .

Measurements

The $[\text{H}^+]$ of the solutions was determined by measurement of the electromotive force of the cell, $E = E^\circ + Q \log[\text{H}^+] + E_j$. E° , Q , E_j and $K_w = ([\text{H}^+][\text{OH}^-])$ were obtained as described previously [41]. The term pH is defined as $-\log[\text{H}^+]$. The value of K_w was found equal to $10^{-13.80} \text{ M}^2$.

The potentiometric equilibrium measurements were carried out using 20.00 mL of $\sim 2.50 \times 10^{-3} \text{ M}$ ligand solutions diluted to a final volume of 30.00 mL, in the absence of metal ions and in the presence of each metal ion for which the $C_M:C_L$ ratios were 1:1 and 1:2. A minimum of two duplicate measurements was taken.

Calculation of equilibrium constants

Overall protonation constants, β_i^{H} , were calculated by fitting the potentiometric data obtained for the free ligand to the HYPERQUAD program [47]. The stability constants of the various species formed in solution were

obtained from the experimental data (potentiometric titrations) corresponding to the titration of solutions of ligands and different metal ions (in different metal:ligand ratios), also using the HYPERQUAD program. The initial computations were obtained in the form of the overall stability constant values, $\beta_{M_mH_hL_l}$:

$$\beta_{M_mH_hL_l} = \frac{[M_mH_hL_l]}{[M]^m[L]^l[H]^h} \quad (1)$$

Mononuclear species, ML, MH_iL (*i*=1–4) and MH_{–1}L, were found for most of the metal ions studied with the three macrocyclic compounds (being $\beta_{MH_{–1}L} = \beta_{ML(OH)} \times K_w$). Differences, in log units, between the values of protonated or hydrolyzed and non-protonated constants provide the stepwise reaction constants. The species considered in a particular model were those that can be justified by the principles of coordination chemistry. The errors quoted are the standard deviations of the overall stability constants given directly by the program for the input data, which include all the experimental points of all titration curves. The standard deviations of the stepwise constants, shown in

Table 1, were determined by the normal propagation rules.

Production of ¹⁵³Sm and ¹⁶⁶Ho

¹⁵³Sm (*t*_{1/2} = 46.8 h; $\beta_{\max} = 0.67$ MeV, 34%; 0.71 MeV, 44%; 0.81 MeV, 21%; $\gamma = 0.103$ MeV, 38%) and ¹⁶⁶Ho (*t*_{1/2} = 26.8 h; $\beta_{\max} = 1.85$ MeV, 51%; 1.77 MeV, 48%; $\gamma = 80.6$ keV, 7.5%; 1.38 MeV, 0.90%) were produced by neutron irradiation of isotopically enriched ¹⁵²Sm(NO₃)₃ or natural Ho(NO₃)₃, respectively, as target materials at the ITN Research Portuguese Reactor (RPI). Nitrate targets were prepared from the corresponding oxides. Briefly, 10-mg-sized samples of enriched ¹⁵²Sm₂O₃ or natural Ho₂O₃ were dissolved in conc. HNO₃ (2 mL) and evaporated to dryness. The samples were taken up in 2 mL of 2% HNO₃ (v/v) and again evaporated to dryness in order to obtain the corresponding nitrate forms. Irradiation was typically performed as follows: power, 1000 kW; thermal neutron flux, $\sim 1.2 \times 10^{13}$ n/cm² s; epithermal neutron flux, $\sim 2.6 \times 10^{11}$ n/cm² s. Following irradiation, the ¹⁵³Sm and

Table 1 Protonation constants^{a,b} of ac₃py14, MeP₂py14 and P₃py14, and stability constants^c (log $K_{M_mH_hL_l}$) of their complexes with Ca²⁺ and lanthanide metal ions; *T* = 25.0 °C; *I* = 0.10 M in NMe₄NO₃

Ion	Species	ac ₃ py14		MeP ₂ py14		P ₃ py14	
		MHL	log β_{MHL}	log K_{MHL}	log β_{MHL}	log K_{MHL}	log β_{MHL}
H ⁺	011	10.27 ^b	10.27	10.97	10.97	11.22	11.22
	012	18.17 ^b	7.90	20.22	9.25	20.38	9.16
	013	23.35 ^b	5.18	27.36	7.14	28.18	7.80
	014	25.75 ^b	2.4	32.49	5.13	34.07	5.89
	015	–	–	35.79	3.30	39.08	5.01
	016	–	–	–	< 1	42.90	3.82
Ca ²⁺	101	5.85 ^b	5.85	5.34(2)	5.34	–	–
	111	–	–	14.52(5)	9.18	–	–
	121	–	–	23.13(5)	8.61	–	–
La ³⁺	101	8.93(2)	8.93	16.55(8)	16.55	17.11(4)	17.11
	111	–	–	23.95(5)	7.40	25.32(4)	8.21
	121	–	–	29.36(5)	5.41	31.58(3)	6.26
	131	–	–	34.04(5)	4.68	35.65(3)	4.07
	141	–	–	–	–	39.39(4)	3.74
Sm ³⁺	1–11	1.39(5)	7.54	6.76(8)	9.79	7.97(5)	9.14
	101	9.78(2)	9.78	17.26(6)	17.26	18.87(6)	18.87
	111	–	–	24.72(6)	7.46	27.02(5)	8.17
	121	–	–	29.65(5)	4.93	33.06(4)	6.04
	131	–	–	33.72(6)	4.07	36.83(3)	3.77
	141	–	–	–	–	40.27(5)	3.44
Gd ³⁺	1–11	2.79(3)	6.99	7.84(7)	9.42	9.98(5)	8.89
	1–21	–	–	–3.86(8)	11.70	–0.4(1)	10.38
	101	–	–	16.62(8)	16.62	18.91(6)	18.91
	111	–	–	23.95(7)	7.33	27.10(5)	8.19
	121	–	–	29.11(6)	5.16	33.31(3)	6.21
	131	–	–	33.56(5)	4.45	37.17(2)	3.86
	141	–	–	–	–	40.60(3)	3.43
Ho ³⁺	1–11	–	–	7.35(9)	9.27	9.82(6)	–9.09
	1–21	–	–	–	–	–1.11(9)	10.93
	101	10.31(1)	10.31	16.84(3)	16.84	19.16(5)	19.16
	111	–	–	23.81(3)	6.97	27.32(5)	8.16
	121	–	–	28.78(3)	4.97	33.71(4)	6.39
	131	–	–	32.89(4)	4.11	38.09(4)	4.38
141	–	–	–	–	–	–	–
	1–11	3.38(5)	6.93	8.14(2)	8.70	10.46(5)	8.70
	1–21	–	–	–	–	0.08(6)	10.38

^aRef. [42]

^b*I* = 0.10 M NMe₄NO₃ [41]

^cValues in parentheses are standard deviations in the last significant figures

^{166}Ho activities were measured by a radioisotope calibrator (Aloka, Curimeter IGC-3, Tokyo, Japan) and the radionuclide purity assessed by γ spectrometry with a Ge(Li) detector (Canberra). Typical yields for 3 h of irradiation were 3–4 mCi/mg for ^{153}Sm and 6–7 mCi/mg for ^{166}Ho , values which are suitable for in vitro and biodistribution studies in mice. The targets were reconstituted in H_2O to produce a stock solution for complex preparation.

Radiolabeling procedure

To prepare each radiolanthanide complex, 5 mg/400 μL of ligands were used. The amount of ligand needed to achieve quantitative complex formation was first dissolved in deionized water followed by alkalization. The required amount of ^{153}Sm or ^{166}Ho solutions was added, according to a 1:2 metal-to-ligand molar ratio, and the pH adjusted to 8 with a 1.0 M NaOH solution. Final ligand concentrations were 11.7 $\mu\text{mol}/500 \mu\text{L}$, 8.8 $\mu\text{mol}/500 \mu\text{L}$ and 7.8 $\mu\text{mol}/500 \mu\text{L}$ for $\text{ac}_3\text{py}14$, $\text{MeP}_2\text{py}14$ and $\text{P}_3\text{py}14$, respectively.

Labeling efficiency, kinetics of the chelation reaction and stability evaluation of the radiolanthanide complexes were accomplished by ascending thin layer chromatography (TLC) using the following chromatographic systems: silica gel TLC strips (Polygram, Macherey-Nagel) developed with three different mobile phases: methanol/ H_2O /acetic acid (4:4:0.2) (system A), saline (system B) and acetone/ H_2O /HCl (7:2:1) (system C). Radioactive distribution on the TLC strips was detected using a Berthold LB 505 detector coupled to a radiochromatogram scanner. The $^{153}\text{Sm}/^{166}\text{Ho}$ complexes evaluated by system A migrate with $R_f=0.80$ ($\text{ac}_3\text{py}14$), 0.08 ($\text{MeP}_2\text{py}14$) and 0.09 ($\text{P}_3\text{py}14$), while ionic ^{153}Sm and ^{166}Ho migrate with $R_f=1.0$. The $^{153}\text{Sm}/^{166}\text{Ho}$ complexes evaluated by system B migrate with $R_f=0.08$ ($\text{ac}_3\text{py}14$), 0.08 ($\text{MeP}_2\text{py}14$) and 0.09 ($\text{P}_3\text{py}14$), while ionic ^{153}Sm and ^{166}Ho migrate with $R_f=1.0$. The $^{153}\text{Sm}/^{166}\text{Ho}$ complexes evaluated by system C migrate with $R_f=0.90$ ($\text{ac}_3\text{py}14$), 0.40 ($\text{MeP}_2\text{py}14$) and 0.09 ($\text{P}_3\text{py}14$), while ionic ^{153}Sm and ^{166}Ho migrate with $R_f=0.9$. Colloidal radioactive forms, which could be considered as a mixture of neutral metal complexes and hydroxides, remain at the origin.

In vitro studies

In vitro stability experiments

These were conducted by adding 50 μL of each ^{153}Sm or ^{166}Ho complex to 100 μL of different physiological solutions, namely saline, phosphate buffered saline (PBS, pH 7.4), 0.1 M glycine-HCl (pH 4.0 and 2.0), and human serum. The mixtures were incubated at 37 °C for up to 5 days. At various time points (1, 2, 3, 4, 5 d) an

aliquot of sample was removed and evaluated by TLC analysis, as described above. The percentage of radiochemical impurities was then calculated.

The overall complex charge

The overall complex charge was determined by electrophoresis on paper strips (Whatman no. 1) after exposure to a constant voltage (300 V) in phosphate buffer (pH 7.4) or Tris-HCl buffer (pH 7.4) for 1 h. The radioactive distribution on the strips was analyzed using a Berthold LB 505 detector coupled with a radiochromatogram scanner to determine the migration of the macrocyclic ^{153}Sm and ^{166}Ho complexes.

Lipophilicity

This was assessed through the determination of the octanol/saline partition coefficients (log P values). It was calculated by the “shakeflask” method based on previously established procedures. Thus, 100 μL of each radiolanthanide complex was added to a solution containing 1 mL saline (pH 7.4) (obtained from a saturated octanol solution) and 1 mL of octanol, in triplicate. The resulting solutions were vortexed and centrifuged at 3000 rpm for 10 min. Aliquots of 100 μL were removed from the octanol phase and from the water phase and the activity measured in a gamma counter. The lipophilicity was calculated as the average log ratio value of the radioactivity in the organic fraction and the aqueous fraction from the three samples.

Total human serum protein binding

This was studied by gel filtration, which enables separation of protein-bound metal complexes from free metal or metal complexes owing to the differences in the molecular weight of the protein fractions (> 60,000 kDa) and the low molecular weight fractions associated with the complexes and free metals (< 850 kDa). A sample (100 μL) of each radiolanthanide complex was incubated with 1 mL of human serum, at 37 °C. After 30 min of incubation, samples were taken. The percentage of radioactivity bound to human serum proteins was determined by spotting the samples (100 μL of each incubation mixture) on the top of a 0.9 cm \times 10 cm Sephadex G 25 (Pharmacia) column. Saline was used as eluent. Eluate fractions of 0.5 mL each were collected and the radioactivity measured in a gamma counter (Berthold LB 2111). The percentage of bound radioactivity was calculated relative to a standard of total activity loaded on the column. Simultaneously, another assay was performed using the same experimental protocol in which each radiocomplex was incubated in saline instead of human serum in order to demonstrate the separation of protein-bound fractions from complex fractions.

In vivo studies

Biodistribution

Biodistribution experiments were carried out with groups of 3–5 female mice CD-1 (randomly bred Charles River, from CRIFFA, Spain), weighing approximately 22–25 g. Animals were intravenously injected with 100 μL (MBq) of radiolanthanide complex via the tail vein. Mice were maintained on normal diet ad libitum. At 30 min, 2 h and 24 h post-administration, animals were killed by cervical dislocation. The radioactive dosage administered and the radioactivity in the sacrificed animal were determined by counting in a dose calibrator (Aloka, Curiometer IGC-3). The difference between the radioactivity in the injected and sacrificed animal was assumed to be due to excretion, mainly urinary. Tissue samples of main organs were then removed for counting in a gamma counter (Berthold LB 2111). Blood samples were taken by cardiac puncture at sacrifice. The blood was then centrifuged, the serum was separated and was analyzed by chromatography. Urine samples were also collected at sacrifice. Biodistribution results were expressed as a percent of injected dose per total organ (% ID/organ). For blood, bone and muscle, total activity was calculated, assuming, as previously reported, that these organs constitute 7, 10 and 40% of the total weight, respectively.

Results and discussion

Protonation and stability constants

The acid–base reactions of $\text{MeP}_2\text{py14}$, $\text{P}_3\text{py14}$ and $\text{ac}_3\text{py14}$ have been studied previously [41, 42] and the corresponding protonation constants are summarized in Table 1. The overall basicity of compounds having methylphosphonate arms is very high compared with that of the *N*-acetate derivative, $\text{ac}_3\text{py14}$ (the order followed is $\text{ac}_3\text{py14} < \text{MeP}_2\text{py14} < \text{P}_3\text{py14}$) [41, 42]. This expected increase in the overall basicity of the methylphosphonate derivatives is explained by electrostatic effects and hydrogen bonding formation [42]. Indeed, the electrostatic effect of the double negative charge on the phosphonate groups prevails over the inductive electron-withdrawal effect of these groups, making the nearby amine more basic [42, 48]. However, the multiple hydrogen-bond, which can be formed, also plays an important role [42, 49]. The different overall basicity of the studied ligands has a direct repercussion on their complexation properties and, consequently, in their biological applications.

The stability constants of $\text{MeP}_2\text{py14}$, $\text{P}_3\text{py14}$ and $\text{ac}_3\text{py14}$ with lanthanides (La^{3+} , Sm^{3+} , Gd^{3+} and Ho^{3+}) were also studied by potentiometric measurements (Table 1). Only mononuclear species were found for the complexes of the three ligands, namely ML and MLOH species; in certain cases, $\text{ML}(\text{OH})_2$ were also

formed. However, while no protonated species were found for the ligand $\text{ac}_3\text{py14}$, the compounds having methylphosphonate arms form several MH_iL ($i = 1–3$ or 4) complexes as expected. We have checked the possibility of formation of other species, but they are not formed under our conditions.

As the ligands $\text{MeP}_2\text{py14}$ and $\text{P}_3\text{py14}$ form several protonated complexes with the studied metal ions, the completely deprotonated ML complexes only exist as the main species at pH values up to 8.5, at which pH the species MLOH start to be formed; see Fig. 2.

A decrease of the basicity of a donor center is expected upon coordination to the metal ion, and this decrease should accompany an increase of the strength of the M–L bond. Indeed, the $K_{\text{MH}_i\text{L}}$ values for the studied complexes are similar to those corresponding to the protonation of phosphonate oxygen atoms of the free ligands (K_3^{H} and K_4^{H} for $\text{MeP}_2\text{py14}$ and $K_3^{\text{H}}–K_5^{\text{H}}$ for $\text{P}_3\text{py14}$). However, the values of K_{MHL} and $K_{\text{MH}_2\text{L}}$ are slightly higher than K_3^{H} and K_4^{H} , respectively (except for $\text{Ho}/\text{MeP}_2\text{py14}$), and in general they are quite insensitive to the type of metal ion, suggesting that the protonation occurs in a phosphonate arm that is not coordinated to the metal ion, or occurs in an oxygen of an arm involved in the coordination although not directly coordinated. In this context it is worthwhile to emphasize that the $K_{\text{MH}_2\text{L}}$ values for the ligand $\text{P}_3\text{py14}$ are systematically higher than K_4^{H} , suggesting that at least one arm is not directly involved in the coordination to these metal ions, probably being away from the coordination sphere.

The usual trend of stability constants for lanthanide complexes was found for this series, namely that the lowest value is obtained for the La complexes and the highest one for the Sm or Ho complexes, the different metal complexes with the same ligand presenting very similar values.

The most interesting point concerning the values of Table 1 is the remarkably different behavior between the lanthanide complexes of the compound containing acetate and those containing the phosphonate arms. In fact, the latter compounds exhibit larger values of ML stability constants, presenting almost double the magnitude, than the corresponding acetate complexes. This was not found for the complexes of Ni^{2+} , Cu^{2+} and Zn^{2+} with the same ligands studied previously, for which similar stability constants were found for the acetate and methylphosphonate derivatives [42]. However, the direct comparison of stability constants involving ligands having such different overall basicity can lead to erroneous conclusions, because the competition of metals and protons for the ligands is not taken into account. Unlike stability constants, pM values ($= -\log[\text{M}^{3+}]$) are dependent on the protonation constants. In Table 2 are collected the pM values for the three ligands calculated at different pH values [50, 51].

Table 2 shows that the highest pM values were found for solutions containing the compound with three

Fig. 2 Species distribution curves calculated for the 1:2 (M:L) complexes of Sm^{3+} with the ligands $\text{ac}_3\text{py}14$ (L^1), $\text{MeP}_2\text{py}14$ (L^2) and $\text{P}_3\text{py}14$ (L^3); $C_L = 2 \times 10^{-5}$ M

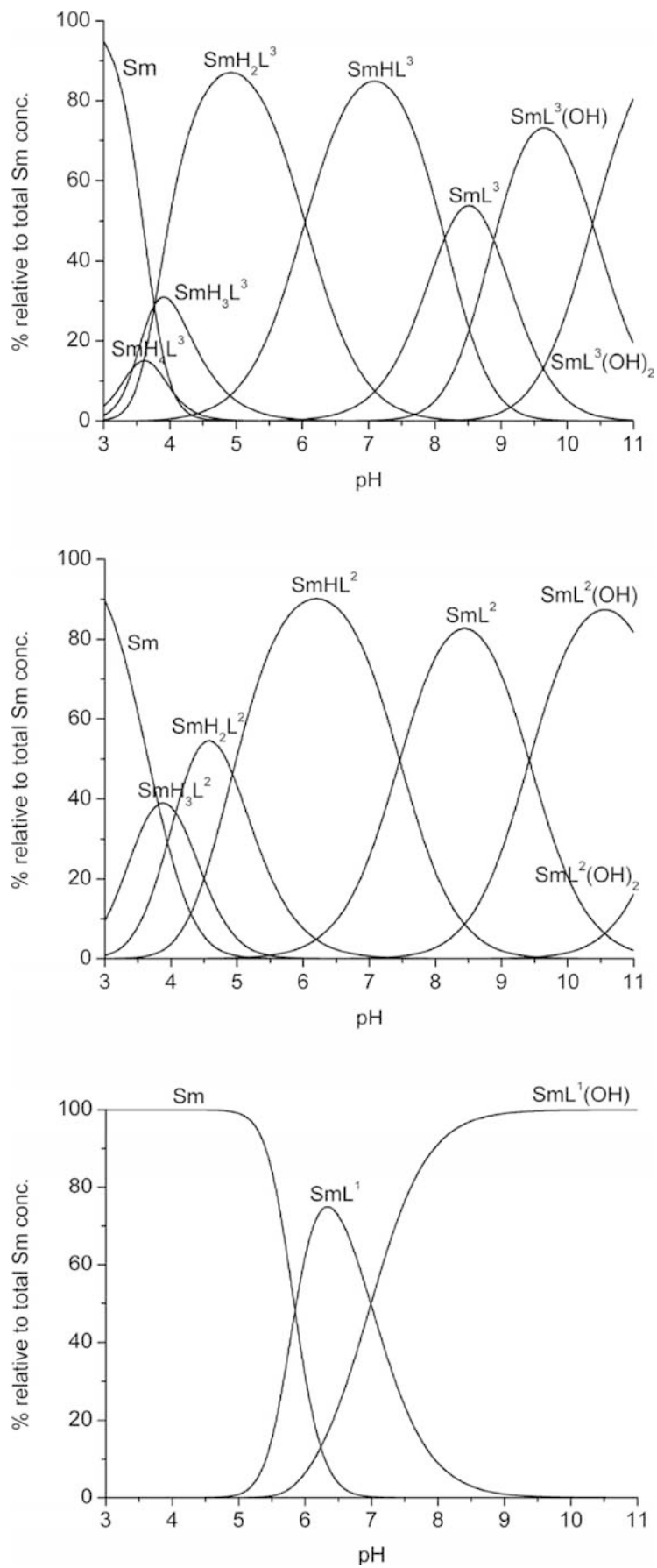


Table 2 pM values^a determined for the complexes of MeP₂py14, P₃py14 and ac₃py14 with some trivalent metal ions; *T* = 25.0 °C; *I* = 0.10 M in NMe₄NO₃ or KNO₃

Ion	Ligand	pH 7.40	pH 9	pH 11
La ³⁺	ac ₃ py14	5.69	9.08	12.31
	MeP ₂ py14	11.23	14.21	17.49
	P ₃ py14	11.87	14.76	18.55
Sm ³⁺	ac ₃ py14	6.84	10.46	13.72
	MeP ₂ py14	11.97	15.00	18.64
	P ₃ py14	13.57	16.64	21.26
Gd ³⁺	ac ₃ py14	–	–	–
	MeP ₂ py14	11.27	14.40	18.07
	P ₃ py14	13.65	16.58	20.73
Ho ³⁺	ac ₃ py14	7.42	11.06	14.30
	MeP ₂ py14	11.37	14.90	18.85
	P ₃ py14	13.89	17.04	21.74

^aValues calculated for 100% excess of free ligand at different pH values; *C*_L = 2.0 × 10⁻⁵ M; *C*_M = 1.0 × 10⁻⁵ M

Table 3 Labelling conditions for ¹⁵³Sm- and ¹⁶⁶Ho-labelled tetraaza macrocycles containing pyridine ligands

Ligand	Reaction conditions		Chelation efficiency (%)	
	¹⁵³ Sm-labelled macrocycles	¹⁶⁶ Ho-labelled macrocycles		
ac ₃ py14	15 min at RT	5 min at RT	~100	~100
MeP ₂ py14	1 h at RT	5 min at RT	~100	~100
P ₃ py14	1 h at RT	5 min at RT	~100	~100

phosphonate arms, followed immediately by those of the ligand with two phosphonate groups, and finally the ligand containing the acetate arms. This means that in these cases the pM and log *K*_{ML} values follow the same trend. As expected, the pM increases with the increase of the pH.

Lukeš et al. [52] found a linear correlation between the thermodynamic stability constants (log *K*_{ML}) of the Gd(III) complexes with linear (edta and dtpa) and cyclic compounds with acetic, phosphonic and phosphinic arms with the sum of the four more basic protonation constants (log *K*₁^H + log *K*₂^H + log *K*₃^H + log *K*₄^H = log β₄^H), following the order phosphinate < acetate < phosphonate. However, all the macrocyclic ligands taken into account for this correlation are 12-membered derivatives (of H₄dota and py12), except H₄trita and H₄teta. Our complexes, together with the values of H₄teta, correlate well with log β₄^H, but with a lower slope and intercept, indicating lower values for the stability constants of the lanthanide complexes of 14-membered derivative ligands.

Table 4 Radiochemical behaviour of ¹⁵³Sm- and ¹⁶⁶Ho-labelled tetraaza macrocycles containing pyridine ligands and free radiolanthanides in the chromatographic systems used in this study

Chromatographic systems	<i>R</i> _f				
	¹⁵³ Sm	¹⁶⁶ Ho	¹⁵³ Sm/ ¹⁶⁶ Ho-ac ₃ py14	¹⁵³ Sm/ ¹⁶⁶ Ho-MeP ₂ py14	¹⁵³ Sm/ ¹⁶⁶ Ho-P ₃ py14
System A	~1.0	~1.0	0.80	0.08	0.09
System B	~1.0	~1.0	0.08	0.08	0.09
System C	0.90	0.90	0.90	0.40	0.09

Radiolabeling

Experimental conditions for the synthesis of ¹⁵³Sm and ¹⁶⁶Ho complexes with pyridine macrocyclic ligands were optimized for chelate concentration, pH and temperature in order to achieve radiochemical purities higher than 98%. The reaction kinetics with ¹⁵³Sm and ¹⁶⁶Ho for ac₃py14, MeP₂py14 and P₃py14 ligands were found to be dependent on chelate concentration and pH. At a 1:1 metal-to-ligand ratio, the labeling reaction was not complete. Maximum complex formation was only achieved at a 2:1 ligand-to-metal ratio. Optimal labeling efficiency over the pH range 7–9 was also observed for all the complexes. However, at pH levels below 7 a decrease in the percentage incorporation of the radiolanthanides was observed. At pH 6, complex formation of ¹⁵³Sm and ¹⁶⁶Ho with ac₃py14 did not occur immediately. Taking into account the species distribution diagram, this result is certainly due to kinetic effects.

The optimized reaction conditions for radiolabeling each ligand with both radiolanthanides and respective chelation efficiencies, expressed as a percentage, are summarized in Table 3. For the ¹⁶⁶Ho complexes the maximum chelation efficiency (>98%) was obtained almost immediately after addition of the radiolanthanide, at room temperature, while the preparation of the corresponding ¹⁵³Sm complexes takes more time, approximately 15 min incubation or about 1 h with the ligands containing acetate or methylphosphonate groups, respectively.

The radiochemical behaviour of each radiolanthanide complex and of the free metals on TLC is summarized in Table 4. Using the three different chromatographic systems A, B and C, it was possible to determine the radiochemical purity since the three expected radiochemical species, ¹⁵³Sm/¹⁶⁶Ho macrocyclic complexes, ionic ¹⁵³Sm/¹⁶⁶Ho, and radioactive colloidal forms, could be identified, except in the case of P₃py14. In the reactions with this ligand it was clear that no ionic ¹⁵³Sm/¹⁶⁶Ho was present, but we were unable to find a chromatographic system that could separate the radiolanthanide complex from the eventual radiochemical colloidal or polymeric species, as also reported for cyclam-based ligands with phosphonic acid arms [53] and organophosphonate complexes [54].

In vitro stability studies

A major concern in the evaluation of radiolanthanide complexes as potential radiopharmaceuticals is their stability under normal physiological conditions. The

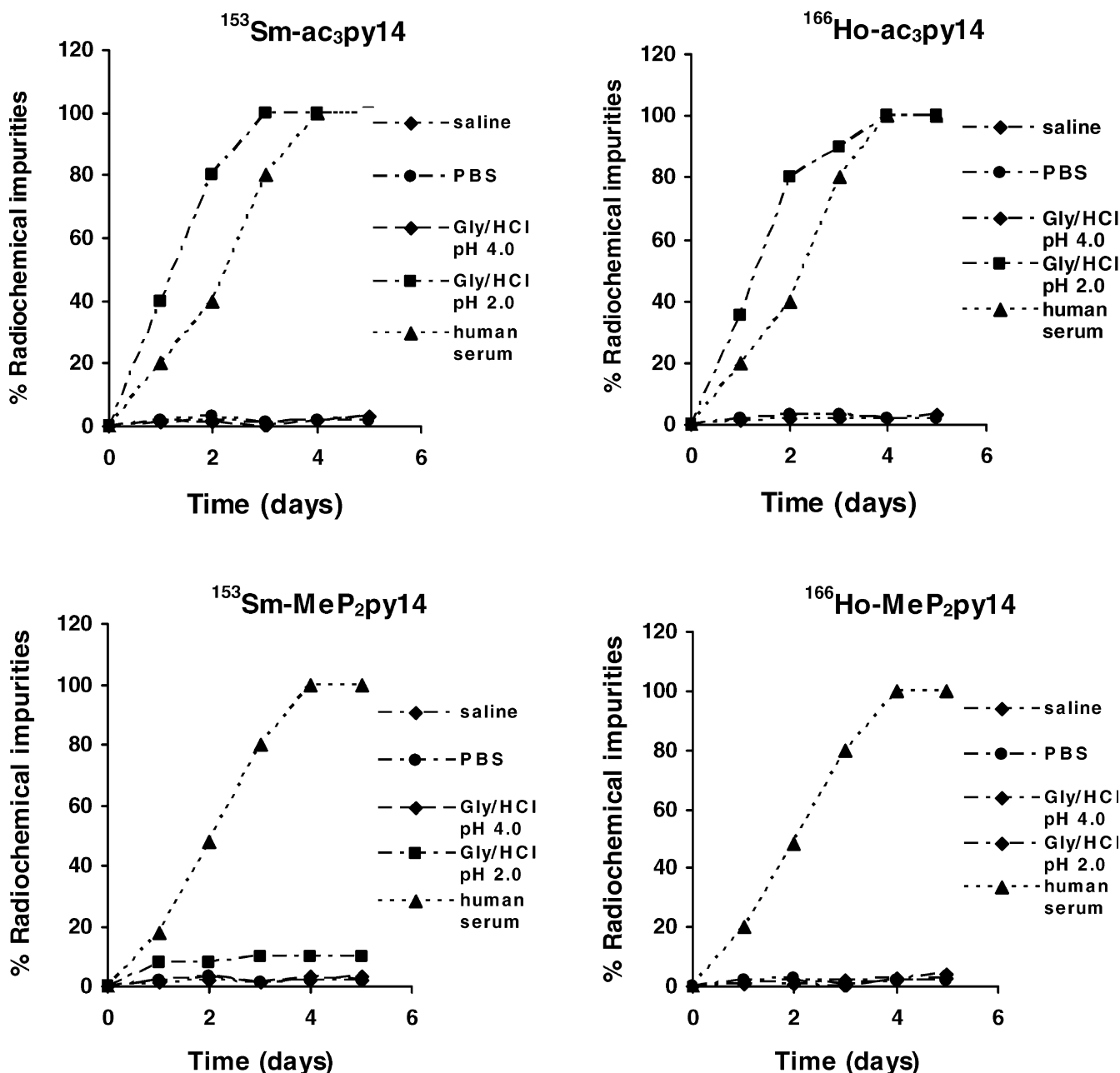
release of radiolanthanides or formation of other radiochemical impurities causes unwanted radiation dose exposure and eventually toxicity in normal tissues and highly limits their clinical efficacy.

All the radiolanthanide complexes prepared were evaluated for in vitro stability in physiological media and human serum over a five-day period at 37 °C. Figure 3 illustrates the results found, as a percentage of radiochemical impurities, when $^{153}\text{Sm}/^{166}\text{Ho}$ -ac₃py14 and $^{153}\text{Sm}/^{166}\text{Ho}$ -MeP₂py14 complexes were

incubated respectively in saline, PBS (pH 7.4), 0.1 M glycine-HCl solution (pH 4.0 and 2.0) and human serum.

From the analysis of the graphics it is clear that the four complexes were stable up to five days in the presence of saline, PBS (pH 7.4), and 0.1 M glycine-HCl solution at pH 4.0, as no significant release of free metal or appearance of radioactive colloidal species could be detected. No radiochemical impurities were also found by incubation with 0.1 M glycine-HCl solution at pH 2.0, with the exception of the radio-complexes with ac₃py14, which are unstable at this acidic pH, releasing free metals. The presence of approximately 40% of radioactivity as free metal was detected after one day of incubation and the total

Fig. 3 In vitro stability of ^{153}Sm and ^{166}Ho complexes with ac₃py14 and MeP₂py14, as a percentage of radiochemical impurities, in saline, PBS (pH 7.4), 0.1 M glycine-HCl solution (pH 4.0 and 2.0) and human serum over time



absence of radioactivity in the R_f corresponding to that complex was found after the third day. The instability of these complexes at pH 2 is in agreement with the observation that at pH < 6 the formation of the radiocomplexes $^{153}\text{Sm}/^{166}\text{Ho-ac}_3\text{py14}$ does not occur (data not shown). Indeed, the distribution species diagram for this ligand, taking into account the stability constants of Table 1, shows that only at pH > 5.8 are the metal ions completely in the complexed form (see Fig. 2).

In the studies performed in human serum, the presence of radiochemical impurities which do not migrate was observed, and this decomposition increases with the incubation time (total decomposition was observed after four days of incubation at 37 °C). Based on TLC analysis, we can say that there are no free ^{153}Sm or ^{166}Ho radiochemical impurities. Whether these species are colloids, such as radiolanthanide hydroxides, or ternary complexes of the type Ln(III)–phosphate–serum proteins, is not clear [38, 55]. In fact, very recently, Neumaier and Rösch [55] have claimed the formation of such ternary radiocomplexes with endogenous phosphate and serum proteins (e.g., albumin) and have also shown how the ionic radius of the Ln^{3+} affects the bound protein. Thus, the radiochemical impurities detected may be related to the dissociation of the initial radiolanthanide complex, which in the presence of human serum proteins may lead to the formation of a ternary complex of this type, which should have a high molecular weight and, consequently, does not migrate under the TLC experimental conditions.

The stability of the radiolanthanide complexes with $\text{P}_3\text{py14}$ was also studied and we did not find any release of free metal over the incubation time, but the possible formation of colloidal forms and/or ternary Ln(III) radiocomplexes could not be detected owing to the lack of an adequate chromatographic system.

Incubation of the radiolanthanide complexes with fresh human blood at 37 °C led to faster decomposition relative to that observed in blood serum. After 30 min the chromatographic analysis of the plasma supernatants presented predominantly radiochemical specie(s) with $R_f \approx 0$. This result indicated that the presence of erythrocytes could be responsible for the fast decomposition of the radiocomplexes. Indeed, competitive displacement of the radiolanthanides by erythrocyte cytoplasmic constituents (e.g., haemoglobin) was also found by other authors [58].

All the pyridine ^{153}Sm and ^{166}Ho radiocomplexes were analysed by electrophoresis to determine the overall charge of the radiolanthanide complexes. These determinations were performed in phosphate and Tris-HCl buffer (pH 7.4, in 0.1 M). All the $^{153}\text{Sm}/^{166}\text{Ho}$ pyridine radiocomplexes remained at the origin, which could indicate a neutral charge for these species. These results do not agree with the expected charge for the $\text{P}_3\text{py14}$ complexes and probably indicate that they are not stable under the electrophoretic experimental conditions.

Partition coefficients

The lipo-hydrophilic character of the $^{153}\text{Sm-py14}$ radiolanthanide complexes was evaluated based on the octanol/saline partition coefficients or log P values (mean values). They are defined as the radioactive concentration of each radiocomplex in the octanol phase and in the aqueous phase at physiological pH (7.4). Data from these determinations can be found in Table 5.

Analysis of these results indicated that all radiolanthanide complexes present high hydrophilic character (log $P < -1$): -1.51 ($\text{ac}_3\text{py14}$), -1.24 ($\text{MeP}_2\text{py14}$) and -1.17 ($\text{P}_3\text{py14}$), probably due to the high degree of ionization of the acetate and phosphonate groups in the complexes.

Total human serum protein binding

When a radioactive complex is administered, like any other drug there is always a fraction bound to the plasma proteins. Protein binding can influence its distribution in the body, its diffusion rate from the vascular compartment, and its rate of elimination, and consequently affects its pharmacokinetics. In an attempt to obtain a better understanding of the biokinetics of our ^{153}Sm complexes, we evaluated their binding to human serum proteins by gel filtration. Data from these determinations are shown in Table 5. Assays performed in parallel to determine the chromatographic behavior of the complexes in the Sephadex G 25 column demonstrated the separation of the protein-bound fractions from the fractions associated with the complexes. After incubation of the radiolanthanide complexes with serum (30 min, 37 °C), 40–60% of the total radioactivity was bound to plasmatic proteins. Taking into account the instability found in vivo, we believe that this binding to human serum proteins may be due to transchelation and/or formation of radiocolloids.

In vivo studies

Although the instability of our radiocomplexes in serum can allow an estimation of the in vivo behaviour [56], we also consider that none of the in vitro studies by themselves can mimic the in vivo environment encountered by the complexes when injected into the blood stream.

Table 5 Percentage of human plasmatic protein binding and lipo-hydrophilic character of ^{153}Sm -labelled tetraaza macrocycles containing pyridine ligands

Ligand	^{153}Sm -labelled macrocycles	
	Human serum protein binding (%)	Lipo-hydrophilic character, log P
$\text{ac}_3\text{py14}$	63	-1.51
$\text{MeP}_2\text{py14}$	51	-1.27
$\text{P}_3\text{py14}$	43	-1.17

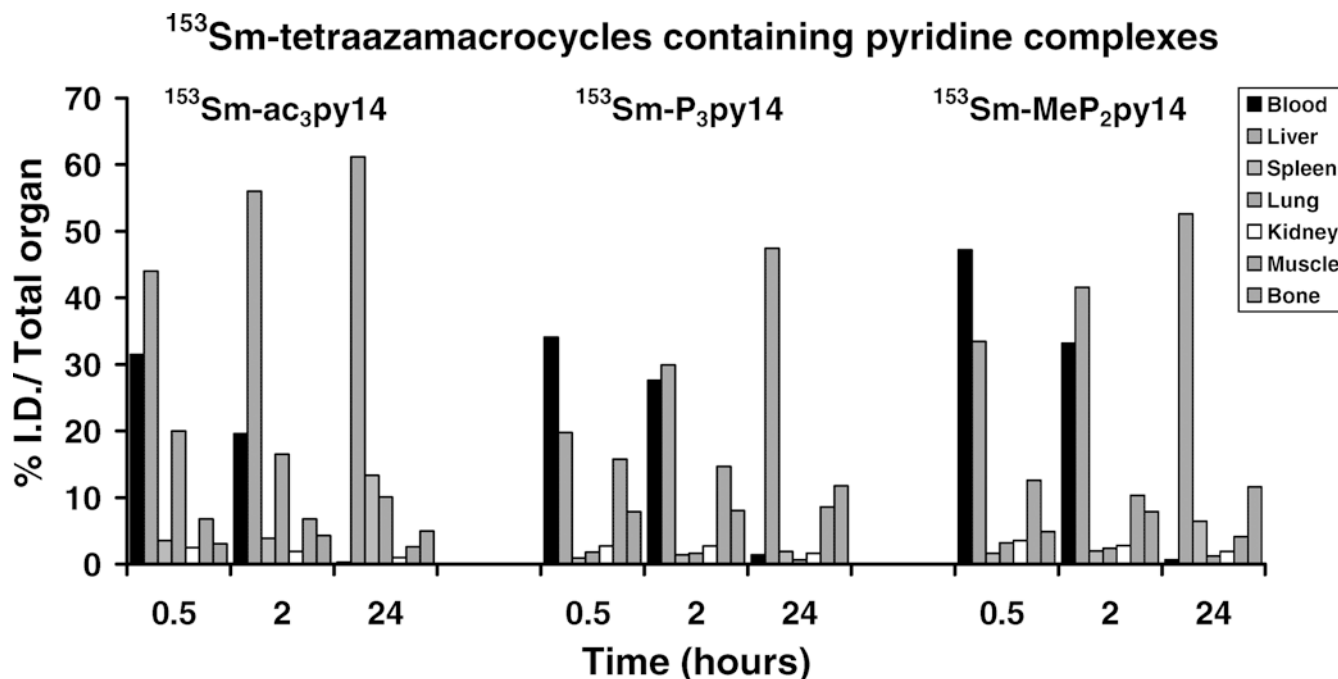
To obtain a much better insight into the nature of the species in the blood after injection, as well as on the nature of the species eliminated by the kidneys, we decided to evaluate the *in vivo* behaviour of the radio-complexes. The biological distribution of ^{153}Sm - and ^{166}Ho -py14 complexes was assessed in CD-1 mice at 30 min, 2 h and 24 h after administration. Tissue distribution data of the radiolanthanide complexes was expressed as a percentage of the injected dose per total organ and the uptake and clearance from most relevant organs can be overviewed in the histograms of Figs. 4 and 5. The total excretion of radioactivity over time is graphically represented in Fig. 6.

Results from these studies indicated a similar pattern for all the radiolanthanide complexes under study, showing a slow clearance from organs like blood and muscle and a very slow rate of total radioactivity excretion from the whole animal body (less than 12% of total injected dose at 24 h after administration). A very high and rapid liver uptake that increases over the time associated with a high hepatic retention of radioactivity was also found. Only a small amount of injected dose is cleared via the liver into the intestines (less than 5% up to 24 h post-administration). The low kidney uptake associated with the low total radioactivity excretion indicated that those complexes almost do not clear through a kidney pathway. Significant spleen and lung uptakes were also observed for some complexes, suggesting the presence of radioactive colloidal/polymeric forms. High accumulation in the spleen that increases

with post-administration time was found in the case of complexes with the $\text{ac}_3\text{py14}$ ligand (^{153}Sm - $\text{ac}_3\text{py14}$: $13.3 \pm 3.4\%$ ID/organ; ^{166}Ho - $\text{ac}_3\text{py14}$: $10.9 \pm 0.8\%$ ID/organ, at 24 h). Significant lung uptake was also observed initially for ^{153}Sm - $\text{ac}_3\text{py14}$ ($20.0 \pm 2.0\%$ ID/organ at 30 min) that decreased over time. Thus, complexes with this ligand seem to be more unstable, leading to the formation of radiochemical species of a colloidal/polymeric nature. Indeed, a tendency to polymerize has also been observed for Ln(III) complexes with polyamino-carboxylate ligands [37]. The main differences in the biodistribution of the different radiolanthanide complexes are related to the rate of clearance from blood and liver uptake as well as the degree of bone uptake. From all the complexes studied, those with $\text{ac}_3\text{py14}$ presented more rapid blood clearance and consequently the fastest accumulation of activity in the liver. This observation may be related to the highest instability of these complexes.

The highest accumulation of radioactivity in bone of the complexes with ligands containing methylphosphonate pendant arms is expected to be due to the binding of these groups to bone hydroxyapatite. In the complexes with $\text{MeP}_2\text{py14}$ and $\text{P}_3\text{py14}$, this accumulation is enhanced over time with the increased number of methylphosphonate groups. However, the complexes containing acetate groups as pendant arms also exhibited a significant bone uptake, especially the ^{166}Ho complex after 24 h (^{153}Sm - $\text{ac}_3\text{py14}$: 3.1 ± 1.0 , 4.3 ± 0.1 and 5.0 ± 0.4 ; ^{166}Ho - $\text{ac}_3\text{py14}$: 6.2 ± 1.0 , 5.9 ± 0.1 and 12.5 ± 0.5 , respectively, at 30 min, 2 h and 24 h). Thus, it is not clear if the observed bone uptake can only be attributed to the presence of ligands with methylphosphonate arms or if it is due to the low stability of the complexes, which promotes the release of the metal

Fig. 4 Biodistribution data, expressed as a percent of injected dose per total organ (% ID \pm SD) of ^{153}Sm complexes with $\text{ac}_3\text{py14}$, $\text{MeP}_2\text{py14}$ and $\text{P}_3\text{py14}$, at 30 min, 2 h and 24 h after *i.v.* administration in female CD-1 mice ($n=3-4$)



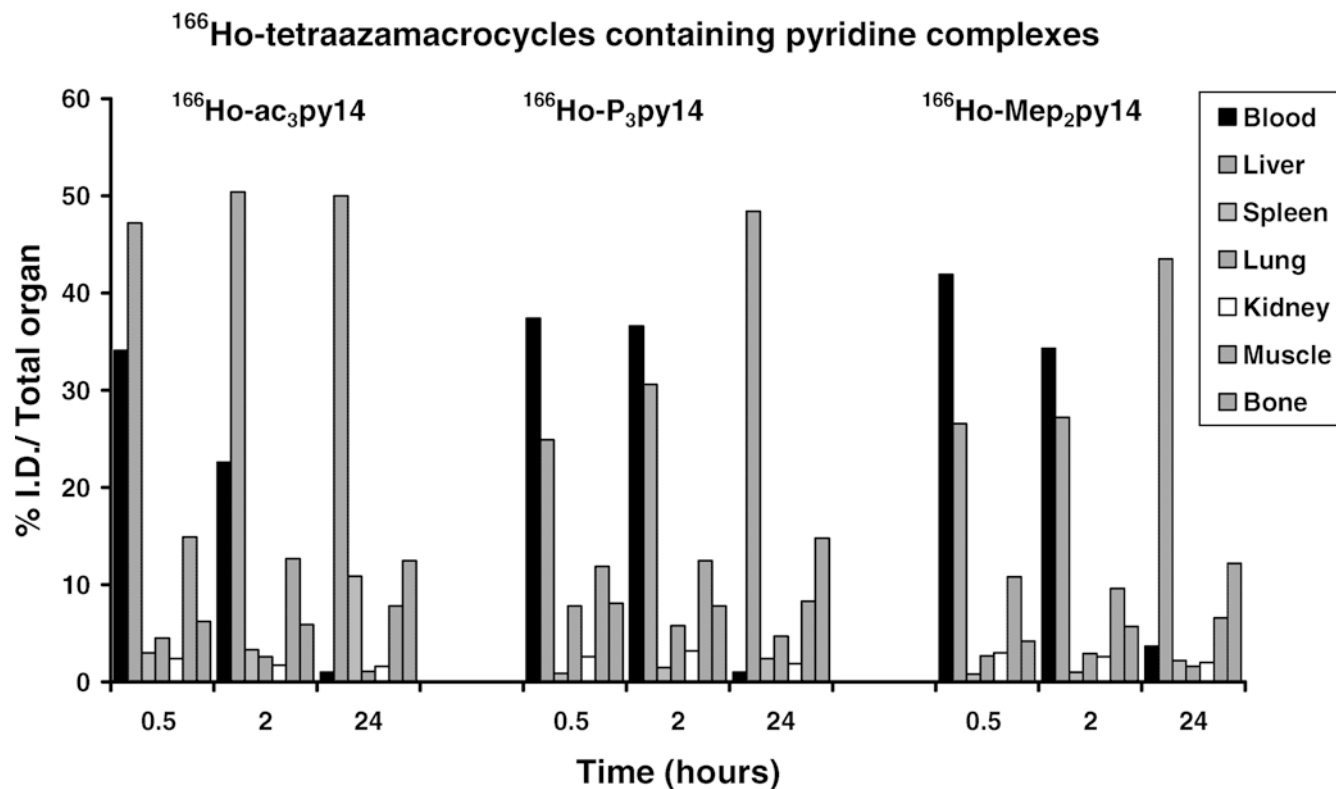


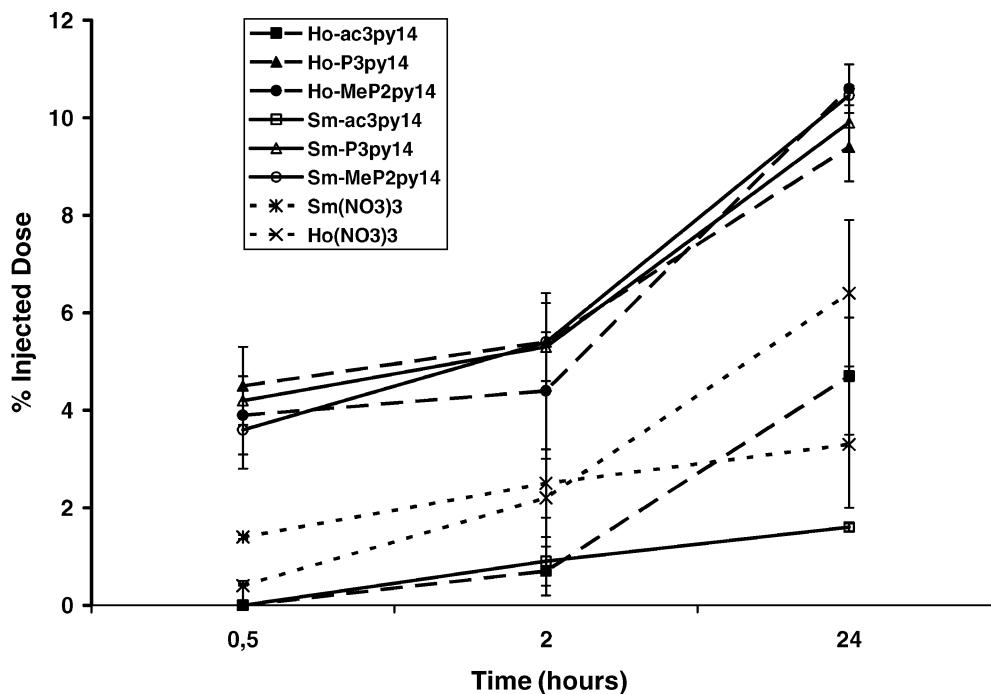
Fig. 5 Biodistribution data, expressed as a percent of injected dose per total organ (% ID \pm SD) of ¹⁶⁶Ho complexes with ac₃py14, MeP₂py14 and P₃py14, at 30 min, 2 h and 24 h after i.v. administration in female CD-1 mice ($n=3-4$)

and leads to its accumulation in bone. Other authors have considered the skeletal and the reticuloendothelial system as the main target organs for the release of heavier and lighter radiolanthanides, respectively [55,

56]. This can probably also justify the bone uptake found by Kim et al. [36] when they studied the in vivo behavior of ¹⁵³Sm complexes with 12-membered pyridine macrocyclic ligands with two methylcarboxylate pendant arms.

In order to obtain a better insight into the in vivo behavior found for our complexes, we carried out some metabolic studies. Samples of urine and mice blood were

Fig. 6 Excretion rate of total radioactivity, expressed as a percent of injected dose of ¹⁵³Sm/¹⁶⁶Ho complexes with ac₃py14, MeP₂py14 and P₃py14, at 30 min, 2 h and 24 h after i.v. administration in female CD-1 mice ($n=3-4$)



collected at sacrifice time, as described above, and analyzed by TLC to determine the extent of complex dissociation. Data from these analyses revealed that none of the radiolanthanide complexes was stable in vivo and different radiochemical species, other than the original radiocomplexes or free metals, were found. The chromatographic system C allowed the identification of a predominant radiochemical impurity in urine and mice serum with a $R_f \approx 0$, while the injected complexes ($\text{ac}_3\text{py14}$, $\text{MeP}_2\text{py14}$) migrate with R_f values of approximately 0.9 and 0.4, respectively. These findings support the hypothesis of in vivo dissociation of the radiocomplexes and the formation of other species, resulting certainly from binding to blood components, like plasma proteins, and/or formation of colloidal species. If dissociation of the complexes tends to occur, it is highly probable that the released radiolanthanide binds to plasma proteins. Besides albumin, it is well known that trivalent lanthanides may behave in vivo similarly to Fe^{3+} . In blood the main carrier protein for Fe^{3+} is transferrin, which also forms complexes with lanthanides [56]. The conditional stability constants for the two binding sites of transferrin with Gd(III) are $\log K_{\text{ML}} = 7.96$ and $\log K_{\text{M}_2\text{L}} = 5.94$ at pH 7.40 and the values for Sm(III) are only slightly higher ($\log K_{\text{ML}} = 8.10$ and $\log K_{\text{M}_2\text{L}} = 5.95$), which will give $\text{pSm} = 8.10$ [57, 58]. These values are very small when compared to the corresponding Fe(III) ones ($\log K'_{\text{ML}} = 20.7$; also at physiological conditions, $\text{pFe} = 20.7$). However, the serum transferrin is not normally saturated with iron, having still some binding capacity for the coordination of other hard metal ions, such as Ln^{3+} . This interaction, although being a possible explanation for the instability of the radiocomplexes prepared with $\text{ac}_3\text{py14}$, does not explain the behavior observed for the other complexes described in this work (Table 2).

In vivo studies with ^{153}Sm and ^{166}Ho nitrate solutions were also performed, using the same animal models, and the tissue distribution evaluated. Since the biological

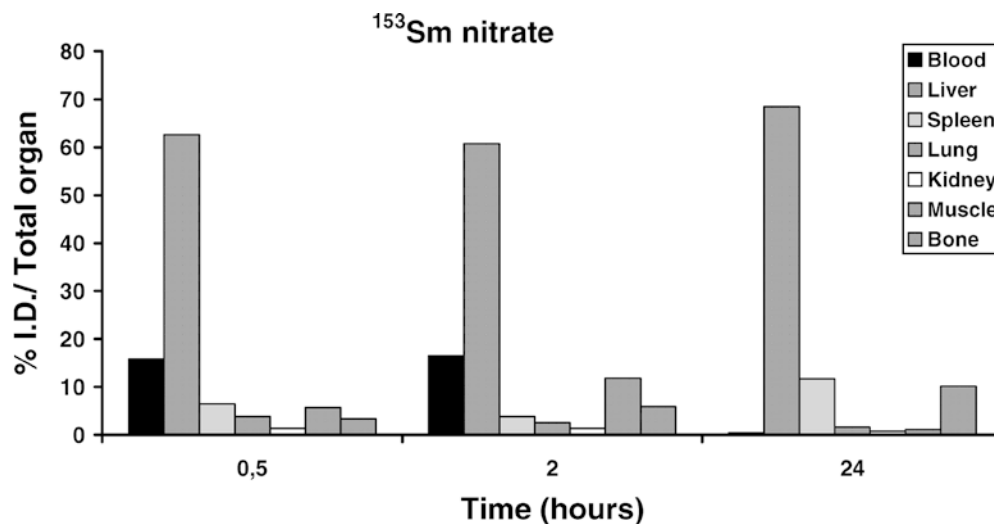
behavior was similar for both radiolanthanides, we only show in Fig. 7 the biodistribution data for $^{153}\text{Sm}(\text{NO}_3)_3$.

The biodistribution profile shows a low excretion of radioactivity and high hepatic uptake. Urine and blood samples were collected at the same time points after administration and analyzed by TLC. Identical chromatographic TLC profiles were observed: the main radiochemical specie(s) present a $R_f \approx 0$ value and no free radiometal could be found. The in vivo behavior of the free radiolanthanides indicated that they form complexes that do not migrate in our analytical systems, which could explain the unexpected low degree of clearance through the kidneys. Probably they form ternary complexes with carrier proteins in blood and/or colloidal forms, as previously described [55]. These results reinforce our previous considerations that the in vivo behavior found for our radiocomplexes does not result from the tissue distribution of them as such, but from the tissue distribution of species which result from their in vivo decomposition.

Conclusions

Potentiometric studies of the tetraaza macrocyclic ligands $\text{ac}_3\text{py14}$, $\text{MeP}_2\text{py14}$ and $\text{P}_3\text{py14}$ with La^{3+} , Sm^{3+} , Gd^{3+} and Ho^{3+} have shown that only mononuclear species are formed, namely ML and MLOH, with protonated MH_iL species also identified with the $\text{MeP}_2\text{py14}$ and $\text{P}_3\text{py14}$ ligands. The ML stability constants found for Ln^{3+} complexes with $\text{P}_3\text{py14}$ and $\text{MeP}_2\text{py14}$ are almost double the values found for the corresponding complexes with $\text{ac}_3\text{py14}$, this trend also being followed by the corresponding calculated pM values. The kinetics and radiolabeling yield of the reactions with ^{153}Sm and ^{166}Ho were maximized at a 1:2 metal-to-ligand ratio and in the pH range 7–9. In general, the complexes are stable in saline, PBS and glycine-HCl solution (pH 4). However, the studies performed with human serum indicated a significant protein bind-

Fig. 7 Biodistribution data, expressed as a percent of injected dose per total organ (% ID \pm SD) of ^{153}Sm nitrate, at 30 min, 2 h and 24 h after i.v. administration in female CD-1 mice ($n = 3-4$)



ing for all the complexes, as well as a high instability. As far as chromatographic studies indicated, the radiochemical impurities formed are not free metals, being certainly either colloidal species or ternary complexes of the type Ln(III)–phosphate–serum proteins. The in vivo behavior of these hydrophilic complexes ($\log P_{o/w}$ range: -1.17 to -1.51) present a slow rate of blood and muscle clearance, presenting also a high liver uptake and a slow rate of total excretion. This profile compares with the biological profile found for the ^{153}Sm and ^{166}Ho nitrates and, according with the low values found for the stability constants and relatively high protein binding, seems to indicate that these radiocomplexes decompose in vivo.

Our results confirm that the rigidity imposed by the pyridine moiety, the cavity size and the number and coordination capability of the pendant arms are important structural features that could be responsible for the low stability constants found for our complexes and for their in vivo instability. These bifunctional chelators are not appropriate for preparing stable lanthanide complexes for targeted radiotherapy. The large size of the lanthanide ions needs the use of ligands with different frameworks and/or pendant arms with higher coordination capability. Attempts to achieve these goals are in progress.

Acknowledgements The authors acknowledge the financial support from Fundação para a Ciência e a Tecnologia (FCT) and POCTI, with co-participation of the European Community fund FEDER (project nos. POCTI/2000/ESP/35877 and POCTI/2000/CBO/35859). This work was also partially supported by COST ACTION D18. K.P.G. also acknowledges Fundação para a Ciência e Tecnologia (FCT) for a grant (SFRH/BD/6492/2001). The authors thank the ITN Research Portuguese Reactor Group for the production of ^{153}Sm and ^{166}Ho .

References

- Hoefnagel CA (1991) *Eur J Nucl Med* 18:408–431
- Hoefnagel CA (1998) *Ann Nucl Med* 12:61–70
- Volkert WA, Goeckeler WF, Ehrhardt GJ, Ketring AR (1991) *J Nucl Med* 32:174–185
- Wessels BW, Mears CF (2000) *Semin Radiat Oncol* 10:115–122
- Volkert WA, Hoffman TJ (1999) *Chem Rev* 9:2269–2292
- Ercan MT, Caglar M (2000) *Curr Pharm Des* 6:1085–1121
- Vallabhajosula S (2001) In: Khalkhali I, Maublant J, Goldsmith SJ (eds) *Nuclear oncology: diagnosis and therapy*. Lippincott Williams & Wilkins, Philadelphia, pp xxx–yyy
- Delaloye AB, Delaloye B (1995) *Eur J Nucl Med* 22:571–580
- Kairemo KJ (1996) *Acta Oncol* 35:343–355
- von Mehren M, Adams GP, Weiner LM (2003) *Annu Rev Med* 54:343–369
- Waldmann TA (2003) *Nat Med* 9:269–277
- Behr TM, Gotthardt M, Barth A, Béhé M (2001) *Q J Nucl Med* 45:189–200
- Froidevaux S, Eberle AN (2002) *Biopolymers* 66:161–183
- Jong M, Kwekkeboom D, Valkema R, Krenning EP (2003) *Eur J Nucl Med* 30:463–469
- Reubi JC (2003) *Endocrinol Rev* 24:389–427
- Deshpande SV, DeNardo SJ, Kukis DL, Moi MK, McCall MJ, DeNardo GL, Meares CF (1990) *J Nucl Med* 31:473–479
- Li M, Meares CF, Zhong GR, Miers L, Xiong CY, DeNardo SJ (1994) *Bioconj Chem* 5:101–104
- Meredith RF, Partridge EE, Alvarez RD, Khazaeli MB, Platt G, Russell CD, Wheeler RH, Liu T, Grizzle WE, Schlom J, LoBuglio AF (1996) *J Nucl Med* 37:1491–1496
- Otte A, Herrmann R, Heppeler A, Behe M, Jermann E, Powell P, Maecke HR, Muller J (1999) *Eur J Nucl Med* 26:1439–1447
- Breeman WA, de Jong M, Visser TJ, Erion JL, Krenning EP (2003) *Eur J Nucl Med Mol Imaging* 30:917–920
- Neves M, Reis MF, Waerenborgh F, Martinho E, Patricio L (1987) *Inorg Chim Acta* 140:359–360
- Neves M, Kling A, Lambrecht RM (2002) *Appl Radiat Isot* 57:657–664
- Bayouth JE, Macey DJ, Kasi LP, Garlich JR, McMillan K, Dimopoulos MA, Champlin RE (1995) *J Nucl Med* 36:730–737
- Dadachova E, Mirzadeh S, Smith SV, Knapp FF Jr, Hetherington EL (1997) *Appl Radiat Isot* 48:477–481
- Fani M, Vranjes S, Archimandritis SC, Potamianos S, Xanthopoulos S, Bouziotis P, Varvarigou AD (2002) *Appl Radiat Isot* 57:665–674
- Ando A, Ando I, Tonami N, Kinuya S, Kazuma K, Kataiwa A, Nakagawa M, Fujita N (1998) *Nucl Med Commun* 19:587–591
- Brenner W, Kampen WU, Kampen AM, Henze E (2001) *J Nucl Med* 42:230–236
- Liu S, Edwards DS (2001) *Bioconj Chem* 12:7–34
- Thöm VJ, Fox CC, Boeyens JCA, Hancock RD (1984) *J Am Chem Soc* 106:5947–5955
- Chang CA, Liu YL, Chen CY, Chou XM (2001) *Inorg Chem* 40:3448–3455
- Izatt RM, Pawlak K, Bradshaw JS, Bruening RL (1995) *Chem Rev* 95:2529–2586
- Anderegg G, Arnaud-Neu F, Delgado R, Felcman J, Popov K (2004) *Journal* (in press)
- Alves FC, Donato P, Sherry AD, Zaheer A, Zhang S, Lubag AJM, Merritt ME, Lenkinski RE, Frangioni JV, Neves M, Prata MIM, Santos AC, de Lima JJP, Geraldes CFGC (2003) *Invest Radiol* 38:750–760
- Banerjee S, Samuel G, Kothari K, Unni PR, Sarma HD, Pillai MRA (2001) *Nucl Med Biol* 28:205–213
- Kim WD, Hrcncir DC, Kiefer GE, Sherry AD (1995) *Inorg Chem* 34:2225–2232
- Kim WD, Kiefer GE, Maton F, McMillan K, Muller RN, Sherry AD (1995) *Inorg Chem* 34:2233–2243
- Aime S, Botta M, Crich SG, Giovenzana GB, Jommi G, Pagliarin R, Sisti M (1997) *Inorg Chem* 36:2992–3000
- Aime S, Botta M, Frullano L, Crich SG, Giovenzana G, Pagliarin R, Palmisano G, Sirtori FR, Sisti M (2000) *J Med Chem* 43:4017–4024
- Aime S, Gianolio E, Corpillo D, Cavallotti C, Palmisano G, Sisti M, Giovenzana GB, Pagliarin R (2003) *Helv Chim Acta* 86:615–632
- Costa J, Delgado R (1993) *Inorg Chem* 32:5257–5265
- Costa J, Delgado R, Drew MGB, Félix V (1998) *J Chem Soc Dalton Trans* 1063–1071
- Guerra KP, Delgado R, Lima LMP, Drew MGB, Félix V (2004) *Dalton Trans* (in press)
- Schwarzenbach G, Flaschka W (1969) *Complexometric titrations*. Methuen, London
- Schwarzenbach G, Biedermann W (1948) *Helv Chim Acta* 31:331–340
- Gran G (1952) *Analyst (London)* 77:661–671
- Rossotti FJ, Rossotti HJ (1965) *J Chem Educ* 42:375–378
- Gans P, Sabatini A, Vacca A (1996) *Talanta* 43:1739–1753
- Geraldes CFGC, Sherry AD, Cacheris WP (1989) *Inorg Chem* 28:3336–3341
- Popov K, Niskanen E, Rönkkömäki H, Lajunen LHJ (1999) *New J Chem* 23:1209–1213
- Alderighi L, Gans P, Ienco A, Peters D, Sabatini A, Vacca A (1999) *Coord Chem Rev* 184:311–318
- Madsen SL, Bannochie CJ, Martell AE, Mathias CJ, Welch MJ (1990) *J Nucl Med* 31:1662–1668
- Lukeš I, Kotek J, Vojtišek P, Hermann P (2001) *Coord Chem Rev* 216–217:287–312

53. Kotek J, Hermann P, Císařová I, Rohovec J, Lukeš I (2001) *Inorg Chim Acta* 317:324–330
54. Popov K, Rönkkömäki H, Lajunen LHJ (2001) *Pure Appl Chem* 73:1641–1677
55. Neumaier B, Rösch F (1999) *Radiochim Acta* 84:201–204
56. Li WP, Smith CJ, Cutler CS, Hoffman TJ, Ketring AR, Jurisson SS (2003) *Nucl Med Biol* 30:241–251
57. Harris WR, Chen Y (1992) *Inorg Chem* 31:5001–5006
58. Chen Y, Harris WR (1999) *Acta Chim Sinica* 57:503–509